

Extracting the R-Wave Position from an FECG Record using Recognition of Multi-channel Shapes

Filip Plešinger, Pavel Jurák, Josef Haláček

Institute of Scientific Instruments of the ASCR, Brno, Czech Republic

Abstract

This study introduces a method for the automatic extraction of the child's R-wave positions from a non-invasive multi-channel fetal ECG (FECG) record (according to the CinC 2013 Challenge).

The method is based on eliminating the influence of the mother's heartbeats, defining the presumed multi-channel shape of the child's R-wave and its recognition in the record. The method is programmed using the C# language. The tested FECG data series were "set A" and "set B" provided by CinC.

1. Introduction

This work is based on the conditions of the CinC Challenge 2013. The goal of the competition is to develop a method for the automatic detection of the fetal QRS complex. The records provided by the challenge are 1-minute long, sampled at a frequency of 1 kHz. The records contain a non-invasive four-channel ECG. Its technical quality varies greatly and record "b15" (with unusable data signals on two channels) was selected for demonstration.

For building this method we decided to extend a self-developed detection framework in view of its natural work with data channels. It is written in the C# language.

Filtering is a common task in the whole process and is not described further.

2. Method

The flowchart of the method is shown in Fig. 1. In the first step, FECG channels are loaded into the memory structure of the framework.

2.1. Eliminating corrupted channels

Poor quality FECG channels can result in a wrong multi-channel shape, for which reason they have to be

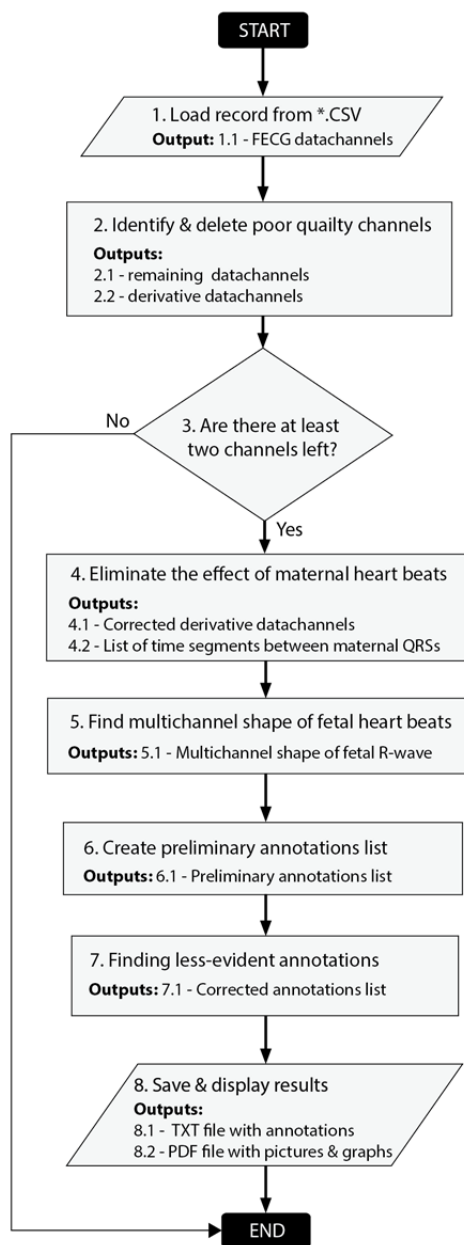


Figure 1. Flowchart of the whole process.

excluded. The number of local extremes is computed to identify corrupted channels.

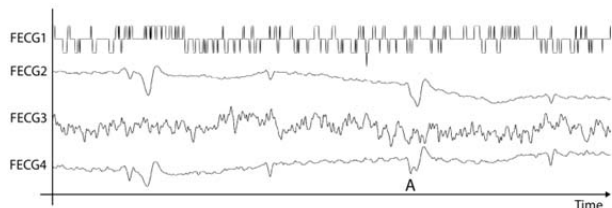


Figure 2. Poor quality four-channel FECG record. The first and the third channel show very low signal-to-noise ratio.

These values are sorted and the two in the middle are taken and an average made. Then the total number of local extremes in each channel (N_E) is compared to this average value (N_{AVG}):

$$(N_E > C_1 \cdot N_{AVG}) \& (N_E < C_2 \cdot N_{AVG})$$

where C_1 and C_2 are empirical constants. When this condition is not met, the values in the tested channel are nullified. If we do not have enough reliable channels after this step, the detection process is skipped and the program ends (Fig. 1, step 3).

2.2. Decreasing the effect of MQRS

The maternal QRS (MQRS) is usually much stronger than fetal QRS (FQRS). When the two overlap at the same time (Fig. 2, A) the MQRS is capable of overshadowing the FQRS completely. We can eliminate this effect partially in signal derivations. For this task detection of maternal QRSs is prepared using thresholds (Fig. 3, MQRS). Next, a list of time segments between each MQRS is assembled.

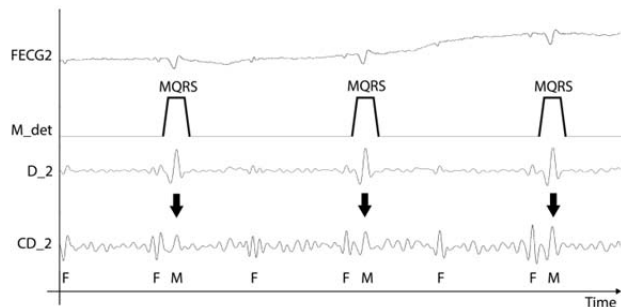


Figure 3. FECG2 channel containing the source signal. M_det holds the response of the MQRS detection algorithm. D_2 contains simple derivative signals. The CD_2 channel holds a derivate signal after decreasing the effect of MQRS (M).

Now we iterate through this list. A shape is defined for each MQRS and for each derivative channel by averaging

5 subsidiary time segments. This shape data structure holds 250 ms before and 350 ms after the start of each MQRS. The averaged shape of MQRSs in each channel is subtracted from the corresponding data channel and stored in a new **corrected derivative** channel (CD). The result is shown in Figure 3. It is clear from Fig. 3 that this process is not strong enough to eliminate the effect of MQRS completely. It is, however, decreased to a level almost similar to the FQRS (compare Fig. 3, F and M).

2.3. The multi-channel shape of FQRS

The concavity/convexity of FQRS peaks is one of the most distinctive elements in FECG records. It can vary over time, but in this case (one-minute records) we assume the concavity/convexity of the FQRS to be stable. We can use this information for simple shape description. If we find the second derivation of the FQRS peak for each channel the **multi-channel shape** (MS) can be stated. The multi-channel shape is, therefore, a numeric array and its length corresponds to the number of FECG data channels. Knowledge of this multi-channel shape allows us to find places with a high probability of FQRS.

Next, we will discuss how to choose positions for reading the convexity/concavity of all channels when building the MS. For this purpose, a **combined score** channel (CS) is created. Its values are based on shape symmetry (horizontal symmetry for FECG, central for derivatives) and the sum of corrected derivative channels.

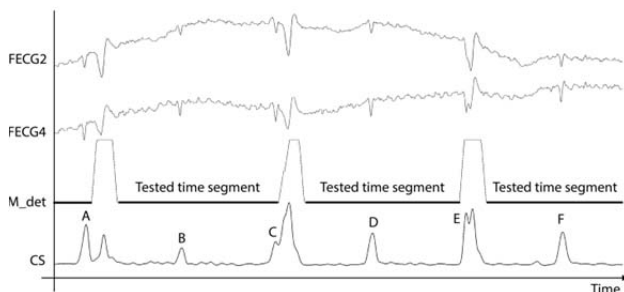


Figure 4. Combined score channel (CS). This responds to corrected derivative channels and to FECG channels.

Next, we iterate through all segments between MQRSs and find the largest peak on the CS. If the peak is unique (in its height) in the tested segment (peaks A, D and F from Fig. 4), then we accumulate the corrected second derivation values into the MS array. The completed **multi-channel shape** array (in the case of the “B15” record) is:

$$MS = \{0, 5.94, 0, 4.85\}$$

This means the FQRS peak is convex on the second and the fourth channel and the values on the first and the third channels are irrelevant (compare with Fig. 2).

2.4. Preliminary annotations list

When the multi-channel shape is known, it is possible to prepare a **Shape Response** channel (SR). This is created by summing the absolute value of the second derivatives of FECG channels in places where its sign corresponds to the adequate sign inside the multi-channel shape.

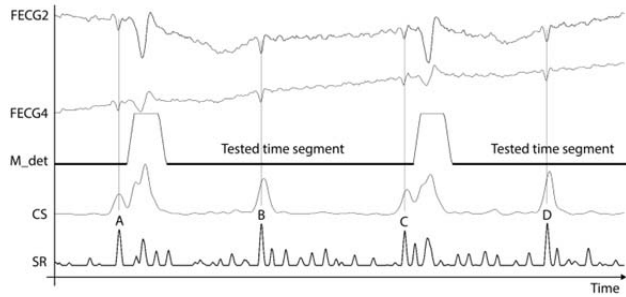


Figure 5. The Shape Response channel (SR). This has the strongest response to the FQRS (A, B, C, D), even if it reacts to a record with two usable channels only.

Next, we can iterate through all segments between MQRS and find the strongest peaks on SR. If the value is at least two times greater than an averaged SR value of the segment, we can find the nearest peak on CS. If these two peaks lie closer together than 30 ms, we have a candidate for FQRS which respects both the symmetry criteria and the shape criteria.

The two highest peaks to the left (H_{PL}) and right (H_{PR}) up to a distance of 300 ms are found and the height of the FQRS candidate (H_{CAN}) can be compared:

$$(C_H \cdot H_{PL} < H_{CAN}) \& (C_H \cdot H_{PR} < H_{CAN})$$

where C_H is an empirical constant. If this condition is met, the FQRS candidate is registered in the **preliminary annotations list**.

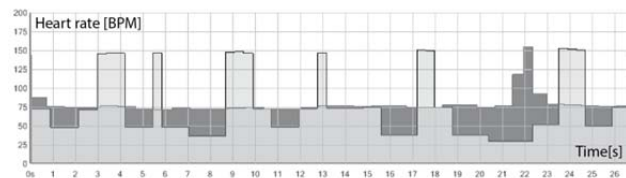


Figure 6. Fetal (light gray) and maternal (dark gray) heart rate based on preliminary annotations list.

The process of creating a preliminary annotations list is extremely strict in order to avoid false FQRS detections. It works only on segments outside the MQRS. The results from the preliminary annotations list cannot be used for fetal heart rate detection yet (Fig. 6.)

2.5. Finding less-evident annotations

FQRSs masked by MQRSs and other less-evident FQRSs are not included in the preliminary annotations list. Our approach to resolving this issue is described further.

2.5.1. Isolated annotations

First we have to find isolated FQRS annotations. This means that the nearest annotations lie further than 550 ms. Next, in the area from 300 to 550 ms, we try to find the distance with the best SR values for both the left and right direction. Then we register two new annotations on the left and right side from the isolated one at the observed distance and iterate further.

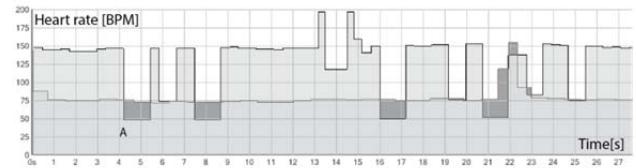


Figure 7. Refined result of fetal heart rate (light gray). The result is more reliable.

2.5.2. Other non-detected annotations

The next part of this task extends continuous groups of annotations to the space where they are missing. This step needs a given number of annotations (a group) and a proper shape in SR to estimate the position of a new one on the left and right side of the group ends. This step is iteratively repeated until it has nothing new to add.

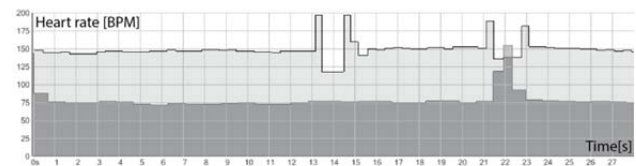


Figure 8. Fetal (light gray) and maternal (dark gray) heart rate after finding missing annotations.

2.5.3. Misidentified FQRSs

When a FQRS is close to a MQRS it can be misidentified. This issue can be easily found and repaired. Generally, when a rapid change of fetal heart rate in an area with a stable heart rate can be found (Fig. 7, A), we assume it is caused by a misidentification.

The issue is corrected by finding a corresponding SR peak in the position based on the previous and (relative) stable heart rate. The result of these operations is shown

in Figure 9. The fetal heart rate is now fully detected and without any significant errors. A detailed view is shown in Figure 10.

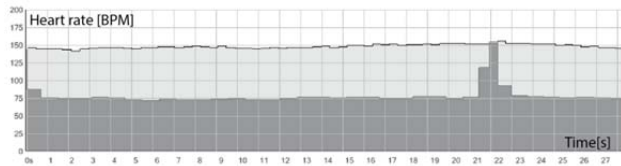


Figure 9. Fetal (light gray) and maternal (dark gray) heart rate in the final form. The only error is badly detected MQRS (22 s) which does not affect the FQRS detection.

3. Displaying the results

When developing this process we run all available records (“a” set and “b” set, provided by the CinC Challenge) in a batch and monitored the effect of changes on all results. The algorithm produces a PDF file (one page for each record) with HR graphs, a few FECG samples and averaged MQRS shapes. We were able in this way to quickly compare the impact of changes on all tested records.

4. Conclusion

We developed a fully automatic method for FQRS detection from multi-channel FECG measurement. It is partially immune to corrupted signals as shown in this article where the used sample has only two usable channels. The algorithm is able to find fetal QRS masked by maternal QRS. The processing time for a one-minute record is below 3 seconds (averaged from total processing time for 100 records on a single core machine at 3.4 GHz including graphics and file output). This processing time makes it usable for a semi-online detection device.

The reliability of the results can be assessed on a number of preliminary annotations (paragraph 2.4.), compared to the total number of annotations.

The processing time can be decreased by parallelizing parts of the algorithm, in particular filtering operations.

Acknowledgements

This work was partially supported by grant no. P102/12/2034 from the Grant Agency of the Czech Republic and by PRECEDENCE CZ.1.05/3.1.00/13.0292 and MEDTECH CZ.1.07/2.4.00/31.0016.

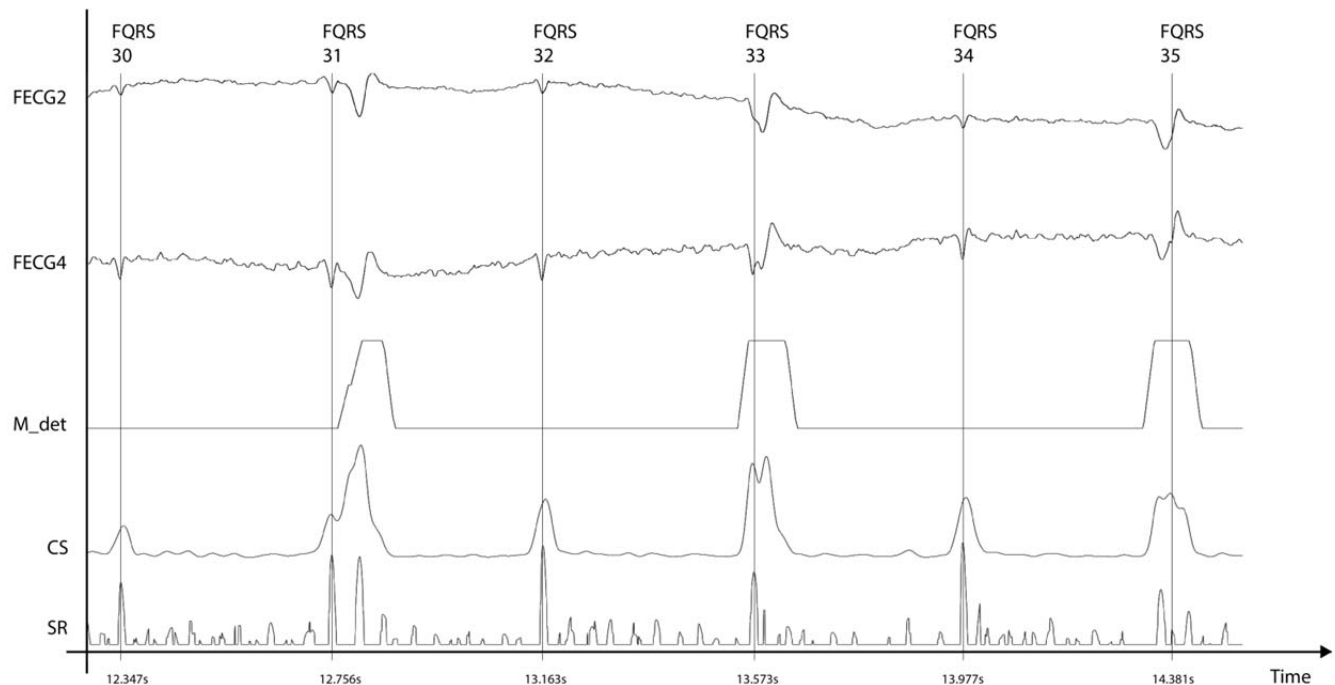


Figure 10. Final results of the developed detection method. Note the masked FQRS annotations number 34 and number 35.

Address for correspondence:
 Filip Plešinger
 Institute of Scientific Instruments of the ASCR, v.v.i.
 Královopolská 147
 612 64 Brno
 Czech Republic
 fplesinger@isibrno.cz